RESEARCH ARTICLE

Autonomous Chiral Microswimmers with Self-mixing Capabilities for Highly Efficient Enantioselective Catalysis

Serena Arnaboldi,[a],[b] Gerardo Salinas,[a] Giorgia Bonetti,[c] Patrick Garrigue,[a] Roberto Cirilli,[d] Tiziana Benincori,[c] Alexander Kuhn*[a]

[a] Dr. S. Arnaboldi, Dr. G. Salinas, P. Garrigue, Prof. Dr. A. Kuhn
Univ. Bordeaux, CNRS, Bordeaux INP, ISM UMR 5255, Pessac, (France)
E-mail: kuhn@enscbp.fr
[b] Dr. S. Arnaboldi
Dip. Di Chimica, Univ. degli Studi di Milano, Milan, Italy
[c] G. Bonetti, Prof. Dr. T. Benincori
Dip. di Scienza e Alta Tecnologia, Univ. degli Studi dell'Insubria, Como, Italy
[d] Dr. R. Cirilli
Istituto Superiore di Sanità, Centro Nazionale per il Controllo e la Valutazione dei Farmaci, Rome, Italy
Supporting information for this article is given via a link at the end of the document.

Abstract: The development of chiral catalysts plays a very important role in various areas of chemical science. Heterogeneous catalysts have the general advantage of allowing a more straightforward separation from the products. One specific case of heterogeneous catalysis is electrocatalysis, being potentially a green chemistry approach. However, a typical drawback is that the redox conversion of molecules occurs only at the electrode/electrolyte interface, and not in the bulk of the electrolyte. The second limitation is that the electrodes have to be physically connected to a power supply to induce the desired reactions. To circumvent these problems, we propose here to replace macroscopic electrodes with an ensemble of self-propelled microswimmers, moving autonomously in solution while transforming simultaneously a prochiral starting compound into a specific enantiomer with a very high enantiomeric excess, accompanied by a significantly increased production rate of the favorite enantiomer.

Introduction

Chiral molecules manifest their peculiarities in different ways in nature. For example, the homochirality of compounds in biochemical systems is of outstanding importance in the pharmaceutical and agrochemical industry. Many enantiopure pharmaceutical compounds are obtained by separation methods, often involving chromatographic columns, or via catalysis.[1] An interesting approach is the use of heterogeneous catalysis to minimize solubility problems and allow a more straightforward purification of the obtained products.[2-4] Electroorganic synthesis employs electrons as reagents, making this methodology very attractive as a sustainable synthetic platform for organic redox reactions.[5-8] However, the success of electroconversion strongly depends on the efficiency of the selective induction of chirality, in synergy with optimized mass transport for a high overall yield. Chemically modified chiral electrodes are a useful tool for asymmetric synthesis, because they only require a small amount of chirality-inducing agents. Nevertheless, they often present as a major disadvantage the poor coverage of the surface with the corresponding chiral selector, thus leading to partially non-stereospecific transformations. An interesting alternative is the use of polymer-coated electrodes for chiral electroorganic synthesis. Abe et al. explored the use of a poly-L-valine-coated graphite cathode for asymmetric electrochemical reductions in two consecutive reports. In the first communication, the asymmetric reduction of prochiral activated olefins was carried out, leading to optical yields of 25% and 43%, respectively.[9] In a second report, the same electrode was used for the asymmetric reduction of prochiral carbonyl compounds with an optical yield of 16.6%.[10] In another work, electrodes coated with a chiral poly-(N-substituted pyrrole)/palladium film, modified with L-(+)-lactic acid moieties as optically active groups, were used for the electrocatalytic hydrogenation of α-keto esters to produce the corresponding hydroxy esters with appreciable enantioselectivities.[11] However, a typical drawback in enantioselective electrocatalysis is that the redox conversion occurs only at the electrode/electrolyte interface, and not in the bulk of the electrolyte. In addition, the electrodes have to be physically connected to a power supply to induce the desired reactions. Herein, we propose to replace the classic macroscopic electrodes with an ensemble of self-propelled microswimmers.

The rational design of micro- and nano-swimmers has gained considerable attention during the last decade,[12-21] due to the increasing number of potential applications in biomedicine,[22-27] environmental remediation,[28,29] (bio)sensing[30,31] and to mimic collective behavior of microorganisms.[32-34] The motion of these devices can be powered either by applying external stimuli (light, ultrasound, and magnetic or electric fields) or by the conversion of chemical energy into motion via different mechanisms, such as Marangoni effect, self-diffusiophoresis, self-electrophoresis and bubble propulsion.[35-45] Recently, the use of self-propelled swimmers as microreactors, coupling the autonomous motion with the possibility to convert a substance “in loco” into a desired product, has been extensively studied. Such dynamic processes, also known as “chemistry on the fly“,[46-48] are based on the synergy between an efficient propulsion and a specific surface functionalization, allowing these mobile platforms to move and actively mix reactants in the solution, combined with a high intrinsic surface reactivity towards the target molecules. This type of microswimmers opens completely new horizons in the frame of chemical synthesis, as they can be considered self-propelled microreactors. In recent years, self-propelled swimmers for “chemistry-on-the-fly” have been introduced for the possible analysis and recognition of chiral information in solution.[49,50]

In fact, scientists are aiming constantly for more innovative designs of these bioinspired objects towards developing self-

propelled devices that can perform various applications from drug delivery, biosensing to a therapeutic treatment of disease target, where actions can be driven easily by different energy sources, including biochemical, optical, magnetic, and electric fields. For example, Escarpa's group designed an autonomous swimmer for "on-the-fly" bio-detection of D- and L-amino acids, taking advantage of the dispersion of the enzymes D- or L-amino acid oxidase.[49] Recently, Muñoz et al. designed a self-propelled Ni@Pt micro-rocket, functionalized with fluorescent CdS quantum dots carrying a chiral host biomolecule, β-cyclodextrin (β-CD).[50] Such micro-rockets work as enantioselective supramolecular cargo platforms in aqueous solution. However, an ex-situ transduction mechanism (optical or electrochemical) is required in order to perform a quantitative analysis of chiral information in solution.

In this context, an interesting approach is to take advantage of the high enantioselectivity of inherently chiral thiophene-based compounds. In inherently chiral molecular material chirality and functional properties originate from the same structural element. As a consequence, the different diastereomeric interactions between the chiral surface and the molecular target in solution lead to thermodynamic difference in redox potential. Thus such molecules can convert selectively only one of the two enantiomers of a chiral analyte at a specific potential value, even when they are present simultaneously in solution.[51] The high specificity of such chiral selectors was exploited to develop e.g. a new approach based on bipolar electrochemistry for the absolute on-off recognition of enantiomers of a chiral probe.[52-55] Recently, these inherently chiral oligomers have also been used to design autonomous enzyme-based swimmers able to produce enantioselective clockwise and anticlockwise motion as function of the enantiomer present in solution.[56] In the present work, we employ these oligomers to design self-propelled asymmetric microswimmers, based on small pieces of zinc (Zn), partially functionalized with one of the antipodes of the inherently chiral material. Theoretically, in acidic media, the oxidation of Zn and the reduction of protons occur spontaneously with a standard redox potential difference of -0.76 V. Due to the large amount of electrons produced by this spontaneous reaction, a considerable fraction can be shuttled from Zn to the inherently chiral oligomer surface. Thus, in the presence of prochiral compounds, their asymmetric reduction allows the selective formation of only one enantiomer, mediated by the inherently chiral material that acts as a catalyst. In addition, the reduction of protons produces enough hydrogen (H_2) on the swimmer surface to induce motion via a bubble propulsion mechanism. Such micro-engines offer considerable promise for accelerating the rate of asymmetric reactions with high yield through enhanced spontaneous micro-mixing, and thus should open up a wide range of practical applications.

Results and Discussion

Initial considerations

Due to their unique ability to selectively oxidize, at a specific applied voltage, the enantiomers of a chiral analyte, inherently chiral materials have gained attention in chiral bipolar electrochemistry for the development of on-off sensors to directly quantify the enantiomeric excesses of unbalanced mixtures of chiral probes.[52,54,55] Furthermore, this concept has been transferred to the field of self-propelled swimmers, to obtain a dynamic read-out of the configuration of chiral analytes through enantioselective trajectories.[52] However, the use of inherently chiral materials in asymmetric electrosynthesis remain a completely unexplored area, with an interesting application potential, considering their high enantiospecificity due to their ability to act as a catalyst to control the stereochemical outcome of the reaction. To study the beneficial effect of employing such inherently chiral materials for asymmetric electrosynthesis, the electroreduction of ketone functions (C = O) to alcohol (–OH) has been chosen as a model reaction. Commonly, the presence of highly reactive functional groups, such as phenyl or carboxyl groups, lead to undesired side products, making the electroreduction of ketones challenging.[57] Acetophenone (AP) and phenylglyoxylic acid (PGA) are suitable candidates since they can be reduced to 1-phenylethanol (1-PE) and mandelic acid (MA), respectively.

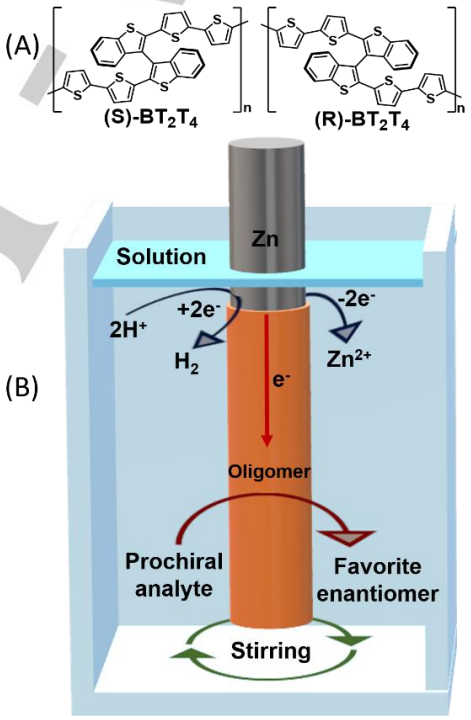

Scheme 1. (A) Inherently chiral structures of the enantiopure antipodes of the (*R*)-BT_2T_4 and (*S*)-BT_2T_4 oligomers. (B) Schematic illustration of the experimental set-up used for the asymmetric synthesis together with the involved redox reactions.

Optimization of the enantioselective electrosynthesis

The enantiopure oligomers of an inherently chiral monomer (Scheme 1A, (*R*)-BT_2T_4 and (*S*)-BT_2T_4, respectively) were deposited galvanostatically on a macroscopic Zn wire's surface, according to a previously described procedure.[52-56] This monomer, with 3,3'-bibenzothiophene as a central unit, has a well-defined electroactivity and can be easily electropolymerized. The two alpha homotopic positions on the thiophene wings guarantee the regioregularity of the oligomerization process. The

high racemization barrier allows the separation of the enantiomers by high performance liquid chromatography (HPLC)[58] on a chiral stationary phase (CSP) under normal phase conditions. Both monomers are stable at room temperature and the chiral features can be fully transferred to the oligomers.[59] Scanning electron microscopy (SEM) analysis, in combination with energy dispersive X-ray spectrometry (EDS) (Figure 1), were used to evaluate the composition and morphology of a Zn wire, functionalized with one enantiomer of the BT_2T_4 oligomer. The deposit appears to be homogeneous with a globular morphology and a thickness of the order of 20 µm (Figure S1). The EDS signal shows that the oligomer modified part has as main components carbon, sulfur and oxygen (orange line), whereas only Zn was detected (grey line) on the pristine part (Figure 1).

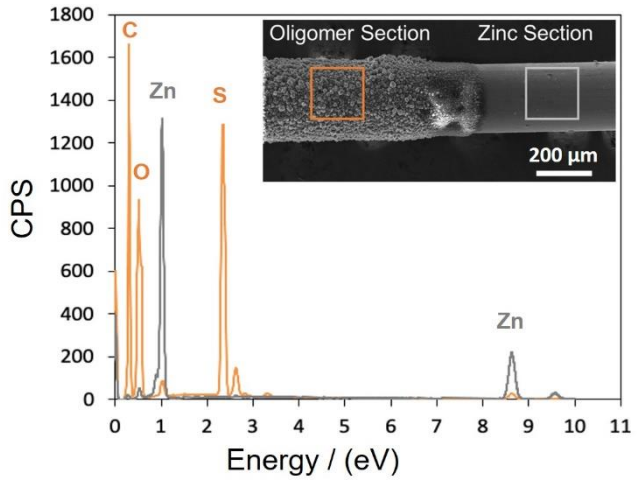

Figure 1. EDS characterization of two selected sections of a Zn wire functionalized with oligomer (orange) and bare Zn (grey). Inset SEM micrograph of the junction between bare Zn and oligomer modified Zn, employed for the enantioselective catalysis.

The possibility of using these modified chiral wires as a reactant for the autonomous stereoselective synthesis of 1-PE was evaluated by immersing 31 mm of the wire (30 mm of enantiopure oligomer modified Zn and 1 mm of pristine zinc) in an aqueous solution of 100 mM AP in 0.5 M H_2SO_4. The general experimental set-up, together with the mechanism of the redox reactions involved in the stereoselective synthesis is illustrated in Scheme 1B. As stated above, oxidation of Zn and reduction of protons take place spontaneously at the bare metal, whereas the stereospecific reduction of the prochiral precursor occurs on the part of the metal wire modified with the enantiopure oligomer. A certain amount of pristine Zn is required to be directly in contact with the solution in order to produce the necessary electron flow from the dissolving metallic Zn to the oligomeric deposit. For the sake of comparison, and to optimize the experimental conditions of the asymmetric synthesis, a pristine wire and two modified Zn wires were used for the initial reduction experiments.

The first tested asymmetric reduction of a prochiral molecule, chosen as a model, was the conversion of AP into one of the two enantiomers of 1-phenyl ethanol (Figure 2A). All three wire samples were kept under constant stirring (60 rpm) for one hour inside the respective solutions containing AP. The products were then extracted with heptane from the reaction mixture and analyzed by enantioselective HPLC on a Chirapak IC CSP column, using a circular dichroism (CD) detector (Figures 2B and 2C).

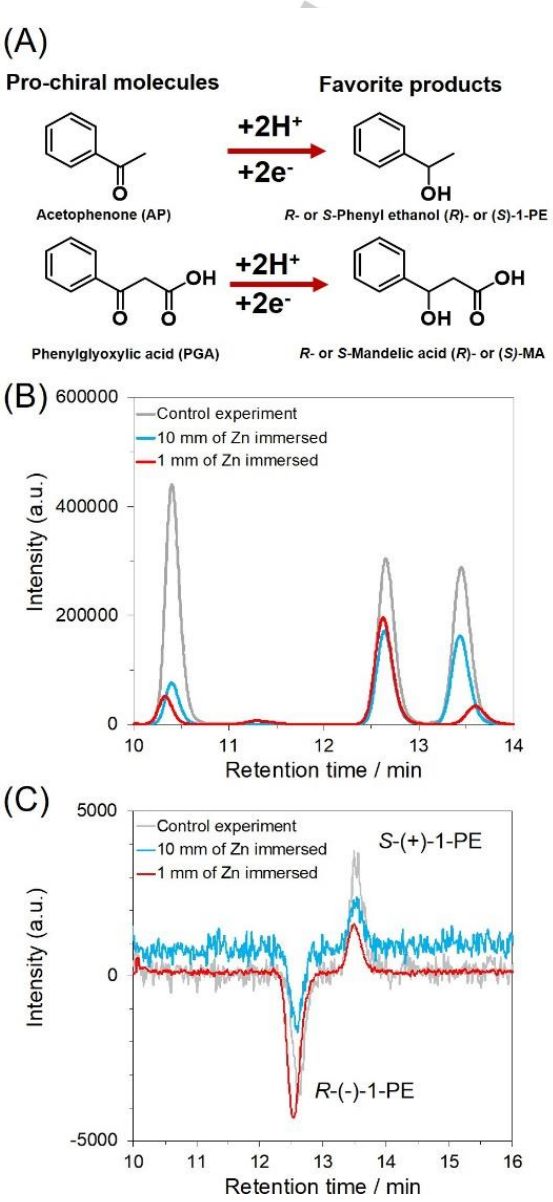

Figure 2. (A) Asymmetric reductions chosen as model reactions. (B) and (C) Chromatograms with online UV/CD detection recorded after the conversion of acetophenone (100 mM) into (*R*)- or (*S*)-1-phenylethanol by soaking in a 0.5 M H_2SO_4 solution: i) 30 mm of the (*R*)-BT_2T_4 oligomer modified wire and 1 mm of bare zinc (red line); ii) 20 mm of the (*R*)-oligomer modified wire and 10 mm of bare zinc (blue line) and iii) 30 mm of a pristine zinc wire (grey line).

When 30 mm of oligomer modified wire and 1 mm of bare Zn are immersed in the reaction medium, AP is successfully reduced to (*R*)-1-phenyl ethanol with a high yield (90%) and an enantiomeric excess (ee) of 85% (Figure 2B red line). This result is confirmed by analyzing the CD chromatograms recorded at a single wavelength during chromatography (Figure 2C), where the first negative signal is related to the preferential production of the (*R*)-enantiomer, followed by the less intense positive signal of the (*S*)-antipode. However, when the same experiment was performed by immersing 20 mm of the wire covered with the (*R*)-oligomer together with 10 mm of bare Zn in the reaction medium, the stereoselectivity of AP reduction drastically decreases (ee < 1 %)

(Figure 2B and 2C blue line). This is due to the large amount of bare Zn immersed in the solution, where AP can be spontaneously reduced on the metal surface in a non-enantiospecific way, leading to a racemic product. As a consequence, the two competing reductions, selective and non-selective, take place simultaneously, but the latter with a higher speed at the bare metal, producing both PE enantiomers in almost equal quantities (product yield of (*R*)-1-PE 41 %, product yield of (*S*)-1-PE 42 %). This was confirmed by a control experiment (Figure 2B and 2C grey lines) where only 30 mm of a bare zinc wire was dipped in the precursor solution. In this case, AP was converted as expected into the two PE enantiomers without any selectivity, leading to a racemic mixture. Therefore, the best way to maximize the product yield during the stereoselective synthesis is to expose only a minimum of bare Zn to the reaction medium.
In the light of these findings, two modified Zn wires were prepared by electrodepositing the two antipodes of the BT_2T_4 oligomer, and immersing them in a 0.5 M sulfuric acid, 100 mM AP solution, with only 1mm of bare Zn and 30mm of modified wire in contact with the reaction medium. The results are depicted in Figures 3A and B. In this way, it was possible to produce preferentially, with a large yield (90%), one or the other PE enantiomer. Perfectly specular chromatograms, with CD detection, were obtained in both cases with an ee value of 85%. This excellent selectivity of the stereospecific synthesis might be explained by the presence of a thin gas layer constantly decorating the fraction of bare Zn, thus preventing this location's unspecific conversion of the prochiral precursor. Consequently, reduction of the starting compound occurs almost exclusively on the part of the metal surface which is modified with the inherently chiral oligomer.

Another parameter, that could influence the efficiency and selectivity of the process, is the thickness of the deposited chiral oligomer, thus different substrates were prepared by modulating the duration of the galvanostatic electropolymerization. The product mixtures of the asymmetric reduction of AP were analyzed by enantioselective HPLC after one hour, and a decrease in selectivity was observed for thinner deposits (Figure S2). This indicates that the reduction of the prochiral molecule take place within the polymer matrix and benefits from the chiral environment, which leads to an increase on the ee. In order to verify the general validity of the proposed concept of autonomous enantioselective redox catalysis, the reduction of phenylglyoxylic acid (PGA) to mandelic acid was chosen as a second model reaction (Figure 2A). The same experimental set-up was used for this synthesis. 30 mm of the wire covered by oligo-(*R*)-BT_2T_4 were immersed, together with 1 mm of bare Zn, in a 100 mM PGA, 0.5 M H_2SO_4 solution. As can be seen from the HPLC analysis (Figure 3C and D), (*R*)-mandelic acid was produced in high yield (88%) with an ee of 79 % demonstrating again the stereospecificity of the process, even in the presence of other functional groups.

Combining stereoselectivity and autonomous motion

As stated above, the spontaneous oxidation of Zn is the main driving force for the reduction of the prochiral molecules on the surface of the inherently chiral monomer. Furthermore, the concomitant bubble formation/release should enable self-propulsion, if the size of the wire is scaled down to smaller dimensions. Therefore, the same strategy of autonomous enantioselective synthesis was followed to design bubble-propelled asymmetric microswimmers. They should not only be able to convert with high selectivity a prochiral compound into its corresponding enantiomer, but also benefit from the continuous renewal of solution at the interface of the swimmer, either by the continuous bubble recoil or by the motion of the device (self-mixing), and thus increase production efficiency. The general design of such microswimmers, with the reactions involved in the stereoselective synthesis, is represented in Scheme 2. After the electrochemical deposition of one BT_2T_4 enantiomer, the functionalized Zn wire was cut into small pieces with an average length of 700 µm ± 400 µm. Scaling down the length of the swimmers, but keeping the diameter identical, might lead to a decrease of %ee, because the amount of wire surface covered by the oligomer becomes comparable with the surface of naked zinc present at the section of the swimmer. However, it is possible to avoid this limitation if not only the length of the swimmers, but also their diameter is decreased simultaneously in order to keep the ratio of polymer-modified and naked surface area constant. Therefore, swimmers with smaller dimensions can in principle be designed by following the same strategy.

From a single wire, two types of swimmers can be produced: Janus type swimmers, with only one bare Zn section, and swimmers with both ends exposing bare Zn (Scheme S1). Since the latter causes an increase in the fraction of metal in direct contact with the solution, one extremity can be isolated with a thin layer of varnish. Consequently, reactions involving the oxidation of the Zn surface will occur only on one side of the swimmer, thus breaking the symmetry of the object and generating motion.

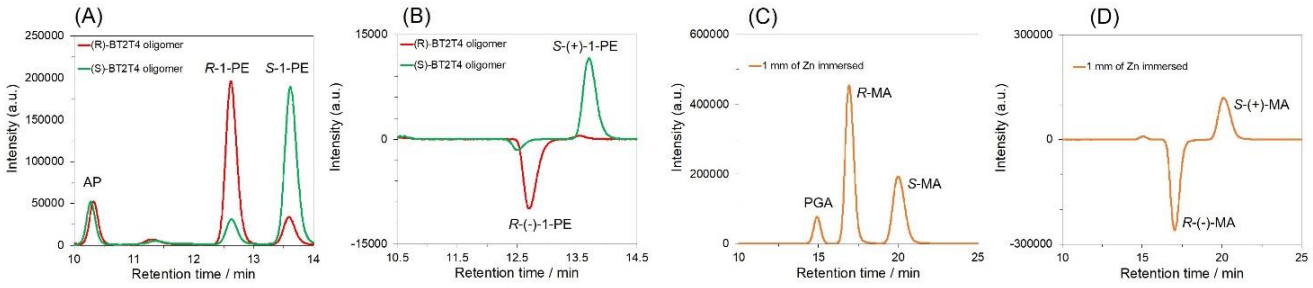

Figure 3. (A) and (B) Chromatograms with online UV/CD detection recorded after the same synthesis as in Figure 2 with 1 mm of bare zinc in contact with the solution, but the wires were functionalized with (*R*)-BT_2T_4 oligomer (red lines) and with (*S*)-BT_2T_4 oligomer (green lines). (C) and (D) Chromatograms with online UV/CD detection recorded after the conversion of 100 mM phenylglyoxylic acid into mandelic acid. The wire was functionalized with (*R*)-BT_2T_4 oligomer and soaked in 0.5 M H_2SO_4 solution.

Scheme 2. General scheme of a bubble-propelled microswimmer, placed at the air/water interface, together with the redox reactions involved in the enantiospecific conversion.

The autonomous motion and stereoselective synthesis achieved with these Janus-type microswimmers were evaluated by placing carefully 15 of these microreactors at the air/water interface of an aqueous solution of 0.5 M H_2SO_4 and 100 mM AP (Video S1). Under these conditions, the reduction of protons by Zn dissolution generates the bubbles responsible for the random motion, whereas the enantioselective reduction of prochiral AP to 1-PE is catalyzed by the surface confined enantiopure oligomers. Such erratic motion is caused by a gradual and irregular consumption of Zn that break the symmetry of hydrogen production on the metal surface. After one hour of self-mixing, the products were extracted with heptane and analyzed by enantioselective HPLC. The same experiment was also carried out with objects functionalized with the enantiopure oligomer having the opposite configuration. Perfectly specular chromatograms were obtained with HPLC (Figure 4A). The enantioselective synthesis occurred with high yields (92%) and with an ee of 90% in both cases. The red line represents the HPLC result for the enantiospecific process catalyzed by the (*R*)-oligomer, leading to (*R*)-1-PE, and the green line stands for the products obtained with the opposite configuration.

Electron Efficiency

Obviously, the reduction of the prochiral starting compound is competing with the production of H_2 and both are consuming zinc. However, by definition at least a certain fraction of electrons has to be devoted to gas bubble formation, otherwise there would be no propulsion. Therefore, the overall efficiency of the reaction strongly depends on the ratio between the concentration of reactant and protons, which needs to be optimized. The formation of the desired product via enantioselective reduction and the bubble propulsion mechanism require a constant supply of protons. Thus, at high pH values (pH ≥ 7), the ketone reduction and bubble formation are strongly limited due to the low availability of protons in the reaction media. Therefore, lower pH values are more favorable. We have performed experiments at higher pH values and the current conditions result from an optimization process. For example, running the experiment at pH = 4 leads to a decrease in selectivity (%ee=70%) and yield (73%). For the optimized pH conditions (pH=0), we have also quantified more precisely the fraction of electrons that are really used for the electrosynthesis. Experiments with the static wire without stirring, and also with the 15 microswimmers, were repeated, and the weight of the zinc wire, and of the microswimmers, were measured before and after the synthesis experiments. This allows estimating the amount of zinc that has been consumed and comparing it with the amount of produced chiral molecules. Calculating the ratio between the moles of alcohol produced after 1 h of reaction and the moles of zinc consumed, we found that the percentage of electrons, specifically used for the enantioselective reduction, is 56 % for the static wire, and 75 % for the microswimmers. This means that in both cases a majority of the electrons is directed towards the organic synthesis (Figure S3). Furthermore, these results demonstrate that self-mixing causes an increase in the percentage of electrons employed for the enantioselective reduction due to an improved mass transport of the prochiral precursor towards the catalytic interface.

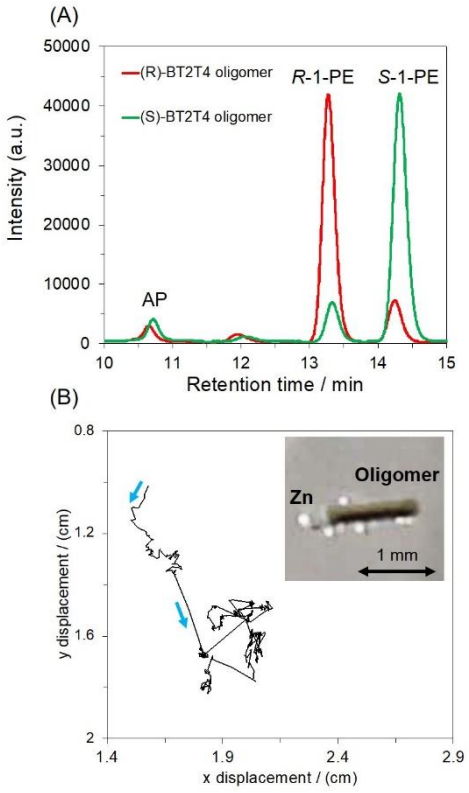

Figure 4. (A) Chromatograms recorded with the product mixtures obtained from the asymmetric synthesis carried out by placing 15 microswimmers, functionalized with (*R*)-BT_2T_4 oligomer (red line) and (*S*)-BT_2T_4 oligomer (green line), in a 100 mM acetophenone 0.5 M H_2SO_4 solution. (B) Trajectory plot of a microswimmer functionalized with the (*R*)-enantiopure oligomer placed in the same solution as in (A), tracked during a time interval of 15 min. The inset shows a close-up of a swimmer indicating bubble formation at the bare Zn surface (left extremity), but also to a smaller extent on the oligomer modified section.

Stereoselective Process Efficiency

The efficiency of the stereoselective process can be compared for three different cases: the chiral wire i) in the absence and ii) in the presence of mechanical stirring (60 rpm), and iii) the 15 autonomous swimmers with self-mixing capability. Considering that the combined length of 15 swimmers is approximatively equal to 10.5 mm and that the length of the previously used chiral wires is 31 mm, the conversion rate of AP, normalized by the active length can be calculated for each experiment (see supporting information for details). This results in 0.11 mmol h^{-1} mm^{-1} and 0.25 mmol h^{-1} mm^{-1} for the chiral wire in the absence and in the presence of mechanical stirring, respectively. Most importantly, the autonomous microswimmers produce the final enantiomer

with a rate of 0.7 mmol h^{-1} mm^{-1}. These values clearly demonstrate a significant improvement in the conversion rate due to the mixing of the solution, inducing a constant supply of educts to the wire.

Since the efficiency is higher with the swimmers, they can be considered as the equivalent of moving microreactors, which are particularly well-adapted to produce the desired enantiomer. The spontaneous random motion leads to active micro-mixing (Figure 4B, Video S1 and S2), thus accelerating the rate of the asymmetric synthesis, and resulting in high yields. This is especially true because the convection occurs all along with the active surface of the oligomer with the same intensity, in contrast to the static chiral wire where the mechanical stirring is not efficient enough to improve mass transport everywhere on the catalyst surface, but mostly only at the bottom of the cell.

Using the same experimental conditions for the enantioselective synthesis, the reaction time was further optimized by analyzing the product mixtures obtained after letting move 15 swimmers, functionalized with (*R*)-oligomer, for different times, ranging from 20 min to 5 h. In Figure S4 the conversion of AP into (*R*)- and (*S*)-phenyl ethanol for the first 1.5 hours is represented. AP is specifically transformed into the favored (*R*)-product, reaching a conversion of 90% after 1 hour. (*S*)-product is also formed in low amounts, with a conversion of 5%. The highest %ee values were obtained after a reaction time of 1 hour (Figure S5). Beyond this time, a decrease in the stereospecificity of the reaction was observed. This is due to the fact that Zn is gradually consumed and the oligomer starts degrading during the synthesis. SEM micrographs of a swimmer, collected from the solution after 2.5 hours show the formation of holes and cracks in the oligomeric substrate (Figure S6). Thus, the solution can infiltrate the oligomer matrix, via the porosity of the film, and reaches the underlying bare Zn surface, causing a more and more pronounced formation of racemic product. This also explains the formation of H_2 bubbles not only at the bare zinc section, but also directly on the oligomer surface (Inset Figure 4B). This observation motivated us to evaluate the reusability of the swimmers by filtrating the product mixture to recover all micro-swimmers. A fresh AP solution (100 mM) was prepared, and then the used swimmers were placed again at the air/water interface for another hour. The product mixture was then analyzed by HPLC to evaluate the enantioselectivity of the process. As expected, a decrease in enantioselectivity was observed, but the discrimination between both enantiomers was still very significant (Figure S7), and the selectivity of the swimmers as a function of the number of recycling loops might be further increased by optimizing the thickness of the oligomer layer.

Conclusion

In this work we have designed asymmetric microswimmers by coupling short fractions of a Zn wire, which spontaneously reduces protons, with inherently chiral oligomers for the enantiospecific electroreduction of acetophenone, chosen as prochiral probe molecule. Motion is triggered by bubble propulsion, accompanied by the transport of electrons from Zn to the inherently chiral oligomer surface. The stereoselective synthesis was first optimized by functionalizing macroscopic Zn wires with the enantiopure oligomers. The fraction of bare Zn immersed in solution, and the thickness of the oligomer deposit are crucial parameters to achieve both, high selectivity and production rate. By changing the conformation of the deposited oligomer it is possible to invert in a specular way the selectivity of the asymmetric process. The concept has also been shown to be of general validity by testing another prochiral starting compound, phenylglyoxylic acid.

The same strategy was then explored to design self-propelled chiral swimmers, acting as moving microreactors, able to convert in an enantioselective way the prochiral educt in solution. An ensemble of micro-swimmers, functionalized with one enantiomer of the inherently chiral oligomer, were placed in a solution containing acetophenone and sulfuric acid. An optimization of the reaction time, to obtain the highest selectivity, was performed by analyzing the conversion of acetophenone into the favorite (*R*)- or (*S*)-alcohol. The highest values were obtained after 1 hour with a product yield of 92 % and an %ee of 90% for both swimmers functionalized with chiral oligomers of opposite conformation. Moreover, and most importantly, the normalized conversion rate of acetophenone, which can be achieved with the microswimmers, is significantly higher compared to what can be obtained with the static wire, and also higher even when the static wire is employed together with mechanical stirring. This clearly indicates the added value of using such mobile micro-reactors in electroorganic synthesis, as they continuously and autonomously stir their local environment, thus ensuring an efficient mass transport of educt towards the swimmer surface.

In conclusion, these original systems appear particularly efficient for asymmetric reductions in order to obtain, with high specificity, the desired enantiopure product with excellent yield. Their performance is enhanced by the fact that the autonomous motion, based on a bubble-propulsion mechanism, induces active micro-mixing, which leads to a more efficient renewal of the prochiral starting compound at the entire catalyst interface. Such an active mixing helps overcoming one of the potential drawbacks of conventional electroorganic synthesis.[5-7] Moreover, since the oligomeric antipodes that constitute the catalytic layer are available in both conformations, it is possible to generate selectively both enantiopure products. Finally, with respect to future applications, these catalytically active autonomous chiral swimmers could be potentially used *en-masse* to scale-up asymmetric reduction processes taking into account that the coated Zn bodies will be consumed by the reaction. For this reason, it will be necessary a study on the modulation of the reaction time as well as a fine tuning of the ratio between reducing agent and substrate.

Acknowledgements

The work has been funded by the European Research Council (ERC) under the European Union's Horizon 2020 research and innovation program (grant agreement n° 741251, ERC Advanced grant ELECTRA). S.A. acknowledges financial support of Università degli Studi di Milano. The authors are also very grateful for fruitful discussions with Patrizia Mussini.

Keywords: Electrosynthesis • inherently chiral oligomers • microswimmers • self-propulsion • heterogeneous catalysis

[1] F. Zaera, *Chem. Soc. Rev*. **2017**, *46*, 7374-7398.

[2] D. Pollock, S. R. Waldvogel, *Chem. Sci.* **2020**, *11*, 12386–12400.

[3] B. Bloom, Y. Lu, T. Metzger, S. Yochelis, Y. Paltiel, C. Fontanesi, S. Mishra, F. Tassinari, R. Naaman, D. H. Waldeck, *Phys. Chem. Chem. Phys*. **2020**, *22*, 21570–21582.
[4] X. Huang, Q. Zhang, J. Lin, K. Harms, E. Meggers, *Nat. Catal*. **2019**, *2*, 34-40.
[5] S. B. Beil, D. Pollok, S. R. Waldvogel, *Angew. Chem. Int. Ed.* **2021**, *60*, 14750–14759.
[6] R. D. Little, *J. Org. Chem*. **2020**, *85*, 13375–13390.
[7] G. Hilt, *ChemElectroChem* **2020**, *7*, 395–405.
[8] T. H. Meyer, I. Choi, C. Tian, L. Ackermann, *Chem* **2020**, *6*, 2484-2496.
[9] S. Abe, T. Nonaka, T. Fuchigami, *J. Am. Chem. Soc*. **1983**, *105*, 3630–3632.
[10] S. Abe, T. Fuchigami, T. Nonaka, *Chem. Lett.* **1983**, *12*, 1033–1036.
[11] N. Takano, C. Seki, *Electrochemistry* **2006**, *74*, 596–598.
[12] J. Wang, *Nanomachines: Fundamentals and Applications*, Wiley, Hoboken, **2013**.
[13] W. Duan, W. Wang, S. Das, V. Yadav, T. E. Mallouk, A. Sen, *Ann. Rev. Anal. Chem*. **2015**, *8*, 311-333
[14] M. Pacheco, M. A. Lopez, B. Jurado-Sanchez, A. Escarpa, *Anal. Bioanal. Chem*. **2019**, *411*, 6561–6573.
[15] F. Novotny, H. Wang, M. Pumera, *Chem* **2020**, *6*, 867-884.
[16] G. Salinas, S. M. Beladi-Mousavi, A. Kuhn. *Curr. Opin. Electrochem*. **2022**, *32*, 100887.
[17] J. Simmchen, L. Baraban, W. Wang, *ChemNanoMat* **2022**, *8*, e202100504.
[18] P. Sharan, A. Nsamela, S. C. Lesher-Perez, J. Simmchen, *Small* **2021**, *17*, 2007403.
[19] G. A. Ozin, I. Manners, S. Fournier-Bidoz, A. Arsenault, *Adv. Mater*. **2005**, *17*, 3011-3018.
[20] A. A. Solovev, Y. Mei, E. Bermudez-Urena, G. Huang, O. G. Schmidt, *Small* **2009**, *5*, 1688-1692.
[21] W. F. Paxton, K. C. Kistler, C. C. Olmeda, A. Sen, S. K. St. Angelo, Y. Cao, T. E. Mallouk, P. E. Lammert, V. H. Crespi, *J. Am. Chem. Soc*. **2004**, *126*, 13424-13431.
[22] R. Lin, W. Yu, X. Chen, H. Gao, *Adv. Healthcare Mater*. **2021**, *10*, 2001212.
[23] L. Kong, J. Guan, M. Pumera, *Curr. Opin. Electrochem*. **2018**, *10*, 174–182.
[24] J. Ou, K. Liu, J. Jianf, D. A. Wilson, L. Liu, F. Wang, S. Wang, Y. Tu, F. Peng, *Small* **2020**, *16*, 1906184.
[25] P. L. Venugopalan, B. E. F. De Ávila, M. Pal, A. Ghosh, J. Wang, *ACS Nano* **2020**, *14*, 9423−9439.
[26] Z. Wu, L. Li, Y. Yang, P. Hu, Y. Li, S. Y. Yang, L. V. Wang, W. Gao, *Sci. Robot*. **2019**, *4*, eaax0613.
[27] Z. Wu, Y. Chen, D. Mukasa, O. S. Pak, W. Gao, *Chem. Soc. Rev*. **2020**, *49*, 8088-8112.
[28] B. Jurado-Sánchez, J. Wang, *Environ. Sci. Nano* **2018**, *5*, 1530-1544.
[29] J. Parmar, D. Vilela, K. Villa, J. Wang, S. Sanchez, *J. Am. Chem. Soc.* **2018**, *140*, 9317−9331.
[30] T. Patino, A. Porchetta, A. Jannasch, A. Llado, T. Stumpp, E. Schaffer, F. Ricci, S. Sanchez, *Nano Lett.* **2019**, *19*, 3440−3447.
[31] K. Yuan, M. A. López, B. Jurado-Sánchez, A. Escarpa, *ACS Appl. Mater. Interfaces* **2020**, *12*, 46588− 46597.
[32] S. Palagi, P. Fischer, *Nat. Rev. Mater*. **2018**, *3*, 113-124.
[33] J. Bastos-Arrieta, A. Revilla-Guarinos, W. E. Uspal, J. Simmchen, *Front. Robot. AI* **2018**, *5*, 97.
[34] L. Baraban, S. M. Harazim, S. Sanchez, O. G. Schmidt, *Angew. Chem. Int. Ed*. **2013**, *52*, 5552-5556.
[35] M. Fernández-Medina, M. A. Ramos-Docampo, O. Hovorka, V. Salgueirino, B. Stadler, *Adv. Funct. Mater*. **2020**, *30*, 1908283.
[36] C. W. Shields IV, O. D. Velev, *Chem* **2017**, *3*, 539-559.
[37] H. Zhou, C. C. Mayorga-Martinez, S. Pane, L. Zhang, M. Pumera, *Chem. Rev*. **2021**, *121*, 4999−5041.
[38] A. D. Ruvalcaba-Cardenas, P. Thurgood, S. Chen, K. Khoshmanesh, F. J. Tovar-Lopez, *ACS Appl. Mater. Interfaces* **2019**, *11*, 39283−39291.
[39] F. Martínez-Pedrero, F. Ortega, R. G. Rubio, C. Calero, *Adv. Funct. Mater*. **2020**, *30*, 2002206.
[40] Y. Sun, Y. Liu, D. Zhang, H. Zhang, J. Jiang, R. Duan, J. Xiao, D. Zhang, B. Dong, *ACS Appl. Mater. Interfaces* **2019**, *11*, 40533−40542.
[41] Q. Wang, R. Dong, C. Wang, S. Xu, D. Chen, Y. Liang, B. Ren, W. Gao, Y. Cai, *ACS Appl. Mater. Interfaces* **2019**, *11*, 6201−6207.
[42] K. Han, C. W. Shields IV, O. D. Velev, *Adv. Funct. Mater*. **2018**, *28*, 1705953.
[43] A. M. Brooks, M. Tasinkevych, S. Sabrina, D. Velegol, A. Sen, K. J. M. Bishop, *Nat. Commun.* **2019**, *10*, 495.
[44] G. Salinas, K. Tieriekhov, P. Garrigue, N. Sojic, L. Bouffier, A. Kuhn, *J. Am. Chem. Soc*. **2021**, *143*, 12708-12714.
[45] S. Palagi, D. P. Singh, P. Fischer, *Adv. Opt. Mater*. **2019**, *7*, 1900370.
[46] E. Karshalev, B. E. F. De Ávila, J. Wang, *J. Am. Chem. Soc.* **2018**, *140*, 3810−3820.
[47] Y. Hu, W. Liu, Y. Sun, *ACS Appl. Mater. Interfaces* **2020**, *12*, 41495−41505.
[48] M. Pacheco, B. Jurado-Sanchez, A. Escarpa, *Chem. Sci*. **2018**, *9*, 8056−8064.
[49] L. Garcia-Carmona, M. Moreno-Guzman, M. C. Gonzalez, A. Escarpa, *Biosens. Bioelectron*. **2017**, *96*, 275-280.
[50] J. Munoz, M. Urso, M. Pumera, *Angew. Chem. Int. Ed.* **2022**, *61*, e202116090.
[51] S. Arnaboldi, T. Benincori, R. Cirilli, W. Kutner, M. Magni, P. R. Mussini, Noworyta, F. Sannicolo, *Chem. Sci*. **2015**, *6*, 1706–1711.
[52] S. Arnaboldi, B. Gupta, T. Benincori, G. Bonetti, R. Cirilli, A. Kuhn, *Anal. Chem*. **2020**, *92*, 10042-10047.
[53] S. Arnaboldi, G. Salinas, G. Bonetti, R. Cirilli, T. Benincori, A. Kuhn, *ACS Meas. Au* **2021**, *1*, 110-116.
[54] G. Salinas, S Arnaboldi, G. Bonetti, R. Cirilli, T. Benincori, A. Kuhn *Chirality* **2021**, *33*, 875-882.
[55] G. Salinas, G. Bonetti, R. Cirilli, T. Benincori, A. Kuhn, S. Arnaboldi, *Electrochim. Acta* **2022**, *421*, 140494.
[56] S. Arnaboldi, G. Salinas, A. Karajic, P. Garrigue, T. Benincori, G. Bonetti, R. Cirilli, S. Bichon, S. Gounel, N. Mano, A. Kuhn, *Nat. Chem*. **2021**, *13*, 1241-1247.
[57] I. Matanovic, *Nat. Catal.* **2019**, *2*, 186-187.
[58] A. Rosetti, G. Bonetti, C. Villani, T. Benincori, R. Cirilli, *Chirality* **2021**, *33*, 146-152.
[59] F. Sannicolò, P. R. Mussini, T. Benincori, R. Cirilli, S. Abbate, S. Arnaboldi, S. Casolo, E. Castiglioni, G. Longhi, R. Martinazzo, M. Panigati, M. Pappini, E. Quartapelle Procopio, S. Rizzo, *Chem-Eur. J.* **2014**, *20*, 15298-15302.

Entry for the Table of Contents

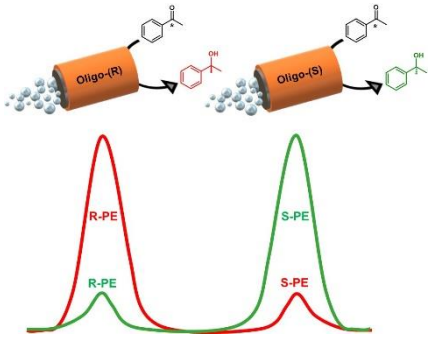

Self-propelled microreactors producing chiral molecules with a high enantiomeric excess are proposed as a complementary approach with respect to classic stereoselective electroorganic synthesis. The straightforward concept is based on a spontaneous redox reaction occurring at the surface of zinc (micro)wires covered with chiral oligomers.